OPEN ACCESS
IOP Publishing
Plasma Sources Science and Technology
Plasma Sources Sci. Technol. **32** (2023) 045002 (13pp)
https://doi.org/10.1088/1361-6595/acc6e9

Effects of a radial variation of surface coefficients on plasma uniformity in capacitive RF discharges

Li Wang[1], Peter Hartmann[2], Zoltán Donkó[2], Yuan-Hong Song[3,*] and Julian Schulze[1,3]

[1] Chair of Applied Electrodynamics and Plasma Technology, Department of Electrical Engineering and Information Science, Ruhr-University Bochum, D-44780 Bochum, Germany
[2] Institute for Solid State Physics and Optics, Wigner Research Centre for Physics, H-1121 Budapest, Konkoly-Thege Miklós str. 29-33, Hungary
[3] Key Laboratory of Materials Modification by Laser, Ion, and Electron Beams (Ministry of Education), School of Physics, Dalian University of Technology, Dalian 116024, People's Republic of China

E-mail: songyh@dlut.edu.cn

Received 8 November 2022, revised 14 February 2023
Accepted for publication 23 March 2023
Published 6 April 2023

Abstract

With the increasing demands toward large area plasma etching and deposition, the radial uniformity of capacitively coupled plasmas (CCPs) becomes one of the key factors that determine process performance in industrial applications. However, there is a variety of parasitic effects, e.g. electromagnetic and electrostatic edge effects, that typically lead to the formation of nonuniform radial plasma density profiles at various discharge conditions with a density peak appearing either at the center or near the edges of the electrodes. Moreover, in commercial CCPs different surface materials are in contact with the plasma at various positions as parts of boundary surfaces such as focus rings, masks, showerhead electrodes, wall and/or target materials. Via complex material specific plasma-surface interactions, the presence of such different surface materials affects plasma uniformity in a way that is typically not understood and, thus, not controlled. In this work, aided by 2d3v graphics processing unit accelerated particle-in-cell/Monte Carlo collision simulations, we study the effects of radial variations of electrode materials on the plasma via their different ion and electron induced secondary electron emission as well as electron reflection coefficients on the discharge characteristics. Based on such fundamental understanding we tailor the radial variation of boundary surface materials to improve plasma uniformity in low pressure CCPs. Such investigations are performed at different neutral gas pressures, where both center and edge high radial plasma density profiles form in the presence of radially uniform surface coefficients that resemble the presence of a single electrode material. It is demonstrated that by radially varying the surface coefficients at the grounded electrode, the radial plasma density profile can be finely adjusted and the plasma uniformity above the wafer placed at the powered electrode can be improved in both cases.

* Author to whom any correspondence should be addressed.

Keywords: geometrically asymmetric CCP, 2D PIC/MCC simulation, surface material variation, plasma uniformity

(Some figures may appear in colour only in the online journal)

1. Introduction

Capacitively coupled plasma (CCP) sources are one of the key tools in the microelectronics industry due to their widespread use in etching, plasma enhanced chemical vapor deposition and sputtering [1, 2]. The properties of the plasmas generated in these sources directly determine the efficiency of the relevant processes and the quality of the products. For instance, ion bombardment at the wafer with controllable energy is essential for high aspect ratio etching with high selectivity, for which, the ion energy distribution function (IEDF) must be tuned through controlling the sheath characteristics [3–6]. In addition, high fluxes of selected neutral radicals are necessary for improving the etch/deposition rate, which relies on the control of the electron energy distribution function (EEDF), since it determines the generation rate of the radicals through the electron impact dissociation reactions of the working gas [7–10]. Moreover, uniform etching and film deposition over a large area become increasingly important to reduce the production costs while keeping a high process quality, which requires the generation of large area and uniform plasmas under specific discharge conditions [11, 12].

Different methods of controlling the plasma properties have been proposed in the last decades. For instance, dual-frequency driven CCPs and the electrical asymmetry effect were studied in detail for realizing the independent control of ion flux and mean energy [13–33]. Various types of tailored voltage waveforms (TVWs) have been demonstrated to provide control of the electron power absorption and the EEDF via modifying the sheath dynamics and its interactions with electrons [34–41]. TVWs were also demonstrated to effectively control the electron velocity distributions at the wafer, through which the positive ion charging inside high aspect ratio dielectric etch features can be compensated by the directed flux of energetic electrons into such structures [42–45]. In addition, by applying an external magnetic field to the discharge, the plasma density can be enhanced and the asymmetry of the plasma can be well adjusted via the magnetic asymmetry effect [46–62]. While these technologies have greatly improved plasma control in CCPs, the uniformity problem in large area commercial reactors remains an issue. In such plasmas driven by high frequencies, the electromagnetic wavelength can be comparable to the reactor diameter and the standing wave as well as the skin effect become evident [63–69]. Moreover, the electrostatic edge effect leads to enhanced electron heating at, e.g. electrode edges, showerhead holes and reactor corners. Finally, the presence of different wall materials can affect the plasma density profile and sheath characteristics via various material specific plasma-surface interactions such as secondary electron emission (SEE), particle reflection, and chemical reactions. All these effects can lead to plasma non-uniformities across large wafers. This remains a prominent problem to be solved in CCPs.

In the past years, several methods to improve plasma uniformity through suppressing electromagnetic effects and/or compensating their effects on the plasma as well as locally controlling the electron heating dynamics have been discussed. The use of lens-shaped dielectrics immersed into electrodes to act as radially varying voltage dividers to avoid non-uniformities and segmenting one large electrode into multiple smaller electrodes were proposed to create a radially uniform vertical electric field and avoid radial non-uniformities due to the standing wave effect [70–73]. Graded conductivity electrodes were proposed in [74], where a metal electrode was covered by a dielectric whose conductivity decreases from the edge to the center, inducing a lower voltage drop across the plasma in the reactor center, which effectively eliminates the standing wave effect. In recent years, structured electrodes, realized by inserting multiple trenches into the grounded counter electrode, were found to locally increase the plasma density by enhancing the electron heating in the trenches. Customizing the electrode topology in this way can, therefore, improve the plasma uniformity above the wafer placed at the powered electrode [75–78]. In addition, the effect of using TVWs and the effect of adding an external electrical circuit to the powered electrode to suppress higher harmonics, on improving plasma uniformity was also reported [67, 79–81].

We note that most of these methods involve modifying the electrode characteristics, i.e. the electrode shape and material. However, one important aspect of such electrode material variations for uniformity control, i.e. the interactions between the surface material and the plasma through effects such as SEE and electron reflection, has hardly been considered so far. Such processes strongly depend on the surface material. In applications of CCP sources in industry, e.g. plasma etching, wafer terminating structures such as focus rings are set at the edges of the wafer. This way the material varies along the radial direction from the wafer to the focus rings, which can lead to different plasma-surface interactions at different radial positions. Similar effects happen due to the presence of various wall, electrode, mask and/or wafer/target materials at different positions inside CCP reactors. Typically such effects are not understood in commercial plasma sources.

Many previous studies have shown that SEE and electron reflection at the reactor surfaces can largely change the discharge characteristics at a variety of discharge conditions [82–84]. Due to the lack of data for realistic surface coefficients, constant secondary electron emission coefficients (SEECs) and electron reflection coefficients, that do not depend on the incident particle energy and material properties, were usually set in plasma simulations in the past. Nevertheless, these studies have shown that the ion induced secondary electrons (γ-electrons) can have significant

influence on the plasma, such as inducing a γ electron heating mode at high pressure and high voltage conditions, changing the quality of the separate control of the ion flux and energy in dual-frequency discharges and even inducing a plasma asymmetry, if different surface materials are used for the powered and grounded electrodes, since the γ-coefficients are different for each surface material [85–88]. Such surface coefficients have been reported to vary strongly depending on the incident particle energy, surface material and the conditions of the surface, such as its roughness and temperature. γ-coefficients ranging from around 10^{-3} to $\sim$1 were reported depending on the incident ion/neutral energy [89]. A total electron induced secondary electron yield (including SEE, electron elastic and inelastic reflection) ranging from 0.03 to more than 3 was reported [90, 91]. From 0 to up to 80% of the electrons can be reflected according to [92]. In recent years, material and energy dependent ion and electron induced SEECs and electron reflection coefficients have been considered in the simulations of CCPs. Several previous works pointed out that the operation mechanism of the discharge and the IEDFs at boundary surfaces can be strongly changed by the material dependent γ-electron emissions [93–97]. The effect of material and energy dependent electron induced secondary electron (δ-electron) emission was studied in detail, a contribution of 51% to the total ionization directly from δ-electrons was found in a geometrically asymmetric discharge at low pressure and high voltage conditions [41, 91, 98]. It was demonstrated in [99] that quantitative agreement between experimental and computational results for various plasma parameters in low pressure CCPs operated in argon gas will only be achieved if specific (realistic) surface coefficients are used in the simulation.

These studies indicate that it is necessary to examine the effects of these surface coefficients on the plasma uniformity, especially because radial surface material variation commonly exists in commercial CCP sources. Moreover, the prominent effect of the material dependent surface coefficients on the discharge also provides a good way to improve the plasma uniformity by radially changing the surface material (of the counter electrode) on purpose. Therefore, in this work we study the effects of a radial variation of SEECs and electron reflection coefficients on the radial plasma uniformity in a geometrically asymmetric CCP reactor based on a 2D graphics processing unit (GPU) accelerated particle-in-cell/Monte Carlo Collision (PIC/MCC) code. Due to the lack of accurate data, i.e. the energy-dependent surface coefficients for a range of different surface materials, in our 'proof of principle' study we use the energy-dependent ion and electron induced SEECs and electron reflection coefficients of SiO_2 as base values and change these radially by multiplying them by a factor ranging from 0 to 2 (resembling the presence of different surface materials qualitatively). In this way, we aim at a qualitative understanding of the effects of radial surface material variations, which are naturally present in many CCP reactors, and examine their potential for improving the plasma uniformity.

The paper is structured in the following way: the 2d3v PIC/MCC simulation method is described in section 2. The effects of the radial surface coefficient variation on the plasma uniformity and the roles of different electron groups generated at the surface via different plasma-surface interaction processes are studied in section 3. Finally, concluding remarks are given in section 4.

2. Computational method

The simulations are conducted with a cylindrical 2d3v (two-dimensional in space and three-dimensional in velocity space) electrostatic PIC/MCC code in argon gas [41, 76]. We consider an electrode configuration, which closely resembles those used in experimental and industrial reactors, see figure 1. The powered and grounded electrodes are indicated by the red and blue lines, respectively. The radius and the thickness of the powered electrode are 12 cm and 1 cm, respectively. The distance between the radial edge of the powered electrode and the grounded guard ring (with a height of 1 cm) is 1 mm. Similar to experiments, the presence of this guard ring suppresses breakdown between the radial edge of the powered electrode and the grounded reactor wall. The thickness of this grounded guard ring is 1 mm and its distance to the reactor sidewall is 2 cm. The gap between the bottom (powered) electrode and the top (grounded) electrode is 5 cm. Since the reactor radius is relatively small, the electromagnetic standing wave effect can be neglected. In addition, as shown in section 3, the highest plasma density in this work is around 8×10^{15} m^{-3}. According to [100], in this case the effective magnetic Reynolds number is smaller than 1 and the skin effect is negligible, too. Therefore, electrostatic PIC/MCC simulations can be used. A single-frequency driving voltage waveform is applied to the powered electrode:

$$V(t) = V_0 \cos(2\pi f t), \tag{1}$$

with a voltage amplitude $V_0 = 300$ V and frequency $f = 13.56$ MHz. The discharge is operated in argon at neutral gas pressures between 0.5 Pa and 5 Pa. The simulation traces electrons and Ar^+ ions. The elementary processes include elastic scattering, excitation to 25 individual levels and ionization collisions between electrons and argon atoms; elastic scattering (including an isotropic and a backward (charge exchange) scattering channel), excitation to three individual levels and ionization collisions between Ar^+ ions and argon atoms. The cross sections of these reactions and more details regarding the treatment of the collision processes in our code can be found in our previous works and some related publications [41, 42, 101–109].

In our study of the effects of the radial variation of surface coefficients on the plasma uniformity, we use the energy dependent ion and electron induced SEECs and electron reflection coefficients of SiO_2 surfaces as a basis. The ion (Ar^+) induced SEEC is shown in figure 2(a) and is adopted from the 'dirty metals' (metal surfaces contaminated by oxygen, water, ambient gas, etc) case as described in [89], where an expression is provided for the ion energy dependence of the secondary electron yield, equation (B15). Although some differences between the SEECs of dirty and oxidized surfaces were found in [110], based on the results given in [111], the effective ion induced SEE of a SiO_2 surface is found to be very

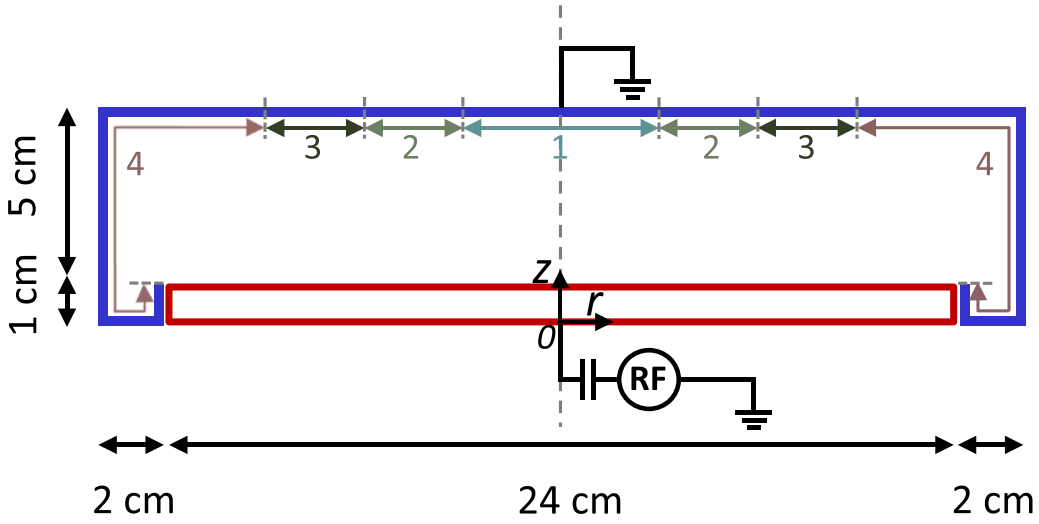

Figure 1. Reactor geometry investigated. The powered and grounded electrodes are represented by the red and dark blue lines, respectively. The grounded electrode is divided into four different radial domains marked by the numbers 1 . . . 4, for which different surface coefficients can be set in the simulation. These regions are: 1: 0 cm $\leqslant r <$ 3 cm, 2: 3 cm $\leqslant r <$ 6 cm, 3: 6 cm $\leqslant r <$ 9 cm and 4: $r \geqslant$ 9 cm. Note, that the last region includes the side wall and bottom segments of the grounded electrode as well.

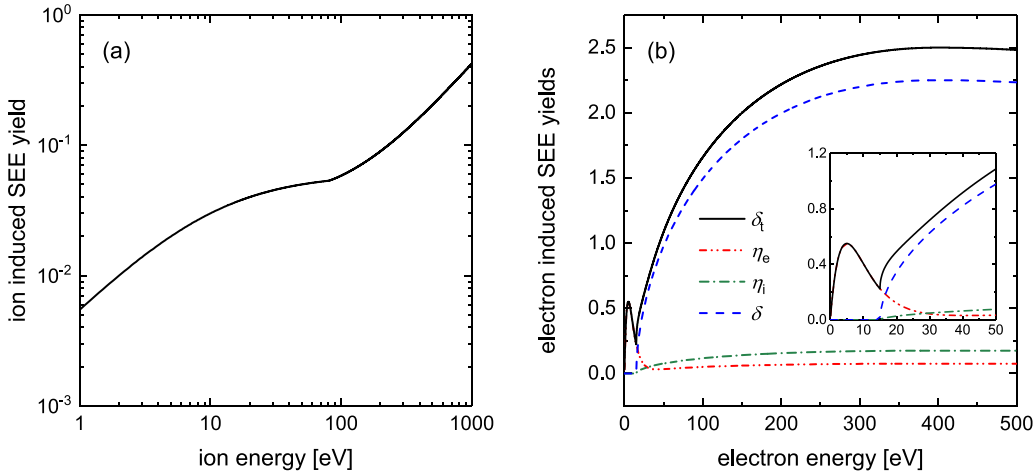

Figure 2. Impact energy dependent electron yields of surface processes included in the simulation: Ar^+ induced secondary electron emission (SEE) for dirty metals [89] (a); and electron induced electron emission processes (elastic reflection, η_e, inelastic reflection, η_i, and electron induced SEE at normal incidence, δ) for SiO_2 surfaces [91] (b).

close to that of dirty metals. In our simulations, we consider three types of electron-surface interactions (see figure 2(b)): elastic reflection, inelastic backscattering, and true secondary emission. The coefficients of these processes depend on the incident energy and angle of the primary electron and the surface properties. Here, we use the model presented in [42, 91, 98] to describe these interactions of electrons with SiO_2 surfaces. According to [89], under the discharge conditions studied here, ion-induced SEE dominates over the contributions of the vacuum ultraviolet (vuv) photon and metastable induced SEE (see figure 12 of [89]). In [112] it was also pointed out that in argon CCPs operated at low pressures, the contribution of metastables to SEE is low compared to argon ions. We therefore neglect the metastable and vuv photon induced SEE processes in our simulations. In the following, we use γ to denote the ion induced SEEC and δ_t to denote the total electron induced electron yield which is the sum of the secondary electron (δ-electron) yield and the elastic as well as inelastic reflection coefficients. As indicated in figure 1, the radial variation of the surface coefficients is realized at the grounded electrode by multiplying γ and δ_t by constant factors for different radial domains. In the simulation, the ion-surface and electron-surface interactions are treated according to the local values of these coefficients. In an experiment this would correspond to an electrode that consists of various concentric rings made of different materials.

Under the conditions studied here ($f = 13.56$ MHz, $V_0 =$ 300 V, 28.4 cm reactor diameter), electromagnetic effects can be ignored and the application of an electrostatic code is justified. The argon gas is assumed to be uniformly distributed in the chamber with a fixed gas temperature of 400 K in our simulations, although a gas flow, determined by the flow rate of the incoming gas and by the positions of the gas inlet(s) and outlet(s) in a commercial CCP may have an effect on the spatial

distribution of the gas density and plasma uniformity. Nevertheless, the results on the effects of radially varying surface materials via their radially changing surface coefficients are assumed to be valid qualitatively also under conditions, where plasma non-uniformities are caused by electromagnetic effects as well as by non-uniform gas distributions, since also under such conditions locally enhanced/reduced surface coefficients will increase/decrease the local plasma density.

In the simulations, 512 to 1024 grid points in the axial direction and 1024 to 1536 grid points in the radial direction are used to resolve the Debye-length. Eight thousand time steps per radio-frequency (RF) period are used to trace even the fastest electrons accurately. In this way all stability criteria of the PIC/MCC scheme are fulfilled. Around 7×10^6 super particles are traced in the simulations for each case. The Poisson equation is solved iteratively using the 'red/black' parallel version of the successive over-relaxation method [113, 114]. We use the Nvidia Compute Unified Device Architecture (CUDA) programming language to perform the simulations. Each particle is assigned to an individual computational thread and all PIC/MCC steps and diagnostic routines are executed in parallel on the GPU. More details regarding the simulation method can be found in our previous works [41, 42].

3. Results

In figure 3, we compare the 2D spatially resolved distributions of the time-averaged electron density, radial electron density profiles at the axial center between the electrodes (at $z = 3.5$ cm) and the corresponding non-uniformity for the cases with uniform SiO_2 surface coefficients and radially varying surface coefficients at the grounded electrode at pressures ranging from 0.5 Pa to 5 Pa. A SiO_2 surface is set and kept unchanged at the powered electrode, i.e. $\gamma = \gamma_{SiO_2}$ and $\delta_t = \delta_{SiO_2}$ at this electrode. To examine whether the plasma uniformity at different pressures can be improved by varying the surface coefficients at the grounded electrode, where no wafer is located in production, this electrode is divided into four regions with different surface materials, i.e. 0 cm $\leqslant r <$ 3 cm, 3 cm $\leqslant r <$ 6 cm, 6 cm $\leqslant r <$ 9 cm and $r \geqslant 9$ cm (including the sidewall). The corresponding surface coefficients are listed in table 1 and are chosen for realizing the best uniformity, but within a realistic range of values for the surface coefficients that can be found for existing materials [89–92]. A single frequency driving voltage waveform is used at $f = 13.56$ MHz with an amplitude of $V_0 = 300$ V.

At 0.5 Pa, a center-high plasma density profile is formed with radially uniform SiO_2 surface coefficients at the grounded electrode. Since the density is relatively low, the large sheaths at the boundaries lead to a rapid decay of the density from the center to the sidewall, resulting in a highly nonuniform density profile. By radially increasing the surface coefficients at the grounded electrode from the center to the edge region, the plasma density at the edges is slightly increased. However, this effect is limited at 0.5 Pa due to the low plasma density, little charged particle bombardment at the electrodes at large radial positions, large electron mean free path and the large sheaths. The low fluxes of electrons and ions to the boundary surfaces at large radial positions result in a low number of emitted and reflected electrons at these positions, which do not cause much ionization close to the boundary surfaces due to their long mean free path. Thus, there is little effect of increasing the surface coefficients at large radii on uniformity. As shown in figures 3(b1) and (c1), the plasma density remains nonuniform across the wafer.

At 0.6 Pa, the nonuniformity is still high in the case of uniform SiO_2 surface coefficients at the grounded electrode. However, the effect of radially increasing γ and δ_t is enhanced due to the reduced electron mean free path and sheath width, for which, the electrons emitted/reflected near the sidewall lead to strong ionization locally without being accelerated far into the reactor center by the sidewall sheath. As a result, the uniformity is largely improved within the domain $r < 8$ cm, as shown in figures 3(a2)–(c2). As will be discussed in detail below, the improvement of the plasma uniformity is mainly induced by the high electron-induced electron yield at the grounded electrode due to the bombardment by high energy electrons. These high energy electrons are mainly accelerated during the sheath expansion at the powered electrode and propagate collisionlessly through the bulk until they hit the opposite electrode. By increasing the gas pressure to 0.7 Pa and 0.8 Pa, the sheath width gets even smaller due to the increased density, leading to a relatively uniform plasma density even without varying the surface coefficients at the grounded electrode. In this case, by radially changing the surface coefficients, the density at the edges can be further increased and the uniformity can be further improved.

We note that increasing the gas pressure can improve the plasma uniformity even without varying the surface coefficients, such as in the case of 1 Pa, at which a good uniformity is achieved with uniform SiO_2 surface coefficients at the grounded electrode. In this case, changing the surface coefficients has only a small effect. However, in industry, the gas pressure is usually fixed according to the specific applications of the CCP source, and changing the gas pressure may cause problems to other plasma characteristics, such as distortion of the IEDF. Therefore, other methods for improving the uniformity, e.g. radially changing the surface material, should be adopted while keeping the gas pressure unchanged. Increasing the gas pressure to 5 Pa, a high density peak appears near the sidewall due to the edge effect, which is largely enhanced in this case by the more local electron kinetic processes. In this case, by reducing the surface coefficients at the edges, i.e. at $r \geqslant 9$ cm, to zero and increasing the surface coefficients in the region 3 cm $\leqslant r <$ 9 cm of the grounded electrode to $1.5\gamma_{SiO_2}$ and $1.5\delta_{SiO_2}$, the density at the edges is reduced and the uniformity is improved, as shown in figures 3(a6)–(c6). At $r <$ 3 cm the surface coefficients are slightly decreased to $0.8\gamma_{SiO_2}$ and $0.8\delta_{SiO_2}$ to reduce the very small density peak in the center region. These results show that through adjusting the surface material, i.e. surface coefficients, at the specific radial regions, the plasma uniformity in different cases can be improved. We note that further increasing the gas pressure to around 8 Pa leads to a more prominent density peak at the edges, while the radially changed surface coefficients show a weak effect

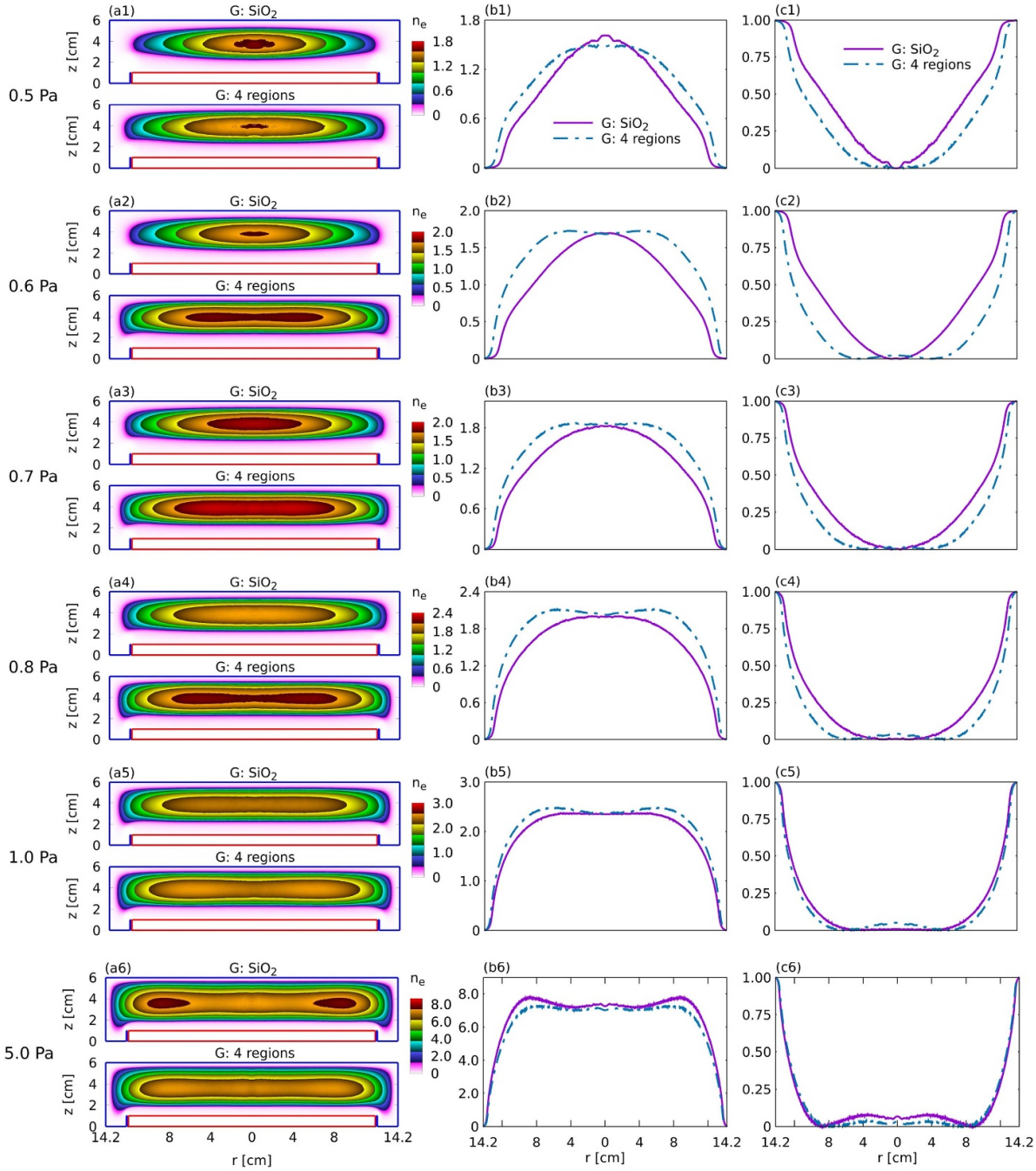

Figure 3. 2D spatial distributions of the time-averaged electron density in units of 10^{15} m^{-3} (first column), radial distributions of the time averaged electron density in units of 10^{15} m^{-3} (second column), and radial nonuniformity $(1 - n_r/n_{max})$ (third column) at $z = 3.5$ cm at different gas pressures with uniform SiO_2 surface coefficients (top plots in a1–a6 and solid lines in b1–b6, c1–c6) and radially varying surface coefficients at the grounded electrode (bottom plots in a1–a6 and dashed lines in b1–b6, c1–c6), respectively. Discharge conditions: single frequency voltage waveform, $f = 13.56$ MHz, $V_0 = 300$ V. G represents the grounded electrode.

at such conditions. In this case, the electron mean free path is largely reduced, for which only a few electrons, that were accelerated by the sheath at the powered electrode, can reach the opposite electrode and bombard it at high energies. Therefore, changing the surface coefficients has little effect on the plasma uniformity. However, this would be changed at even higher pressures, where the γ-mode dominates the discharge. Under such conditions, the surface coefficient variation is expected to again effectively change the plasma uniformity, since it can locally enhance/attenuate the ionization rate by the emission of γ-electrons, which are accelerated towards the bulk by the local sheath electric field and are collisionally multiplied inside the sheath in the γ-mode. Due to the high computational cost for high pressure conditions, studying this effect by 2D PIC/MCC simulations is not easy, but it could be examined by experiments in the future.

Table 1. Ion induced secondary electron emission coefficient γ and total electron induced electron yield δ_t for different radial domains of the grounded electrode. In the table, γ_{SiO_2} and δ_{SiO_2} denote the γ coefficient and total electron induced electron yield for SiO_2, respectively.

p [Pa]	0 cm $\leqslant r <$ 3 cm $\gamma/\gamma_{SiO_2}, \delta_t/\delta_{SiO_2}$	3 cm $\leqslant r <$ 6 cm $\gamma/\gamma_{SiO_2}, \delta_t/\delta_{SiO_2}$	6 cm $\leqslant r <$ 9 cm $\gamma/\gamma_{SiO_2}, \delta_t/\delta_{SiO_2}$	$r \geqslant$ 9 cm $\gamma/\gamma_{SiO_2}, \delta_t/\delta_{SiO_2}$
0.5	0.5, 0.5	1, 1	1.5, 1.5	2, 2
0.6	0.5, 0.5	1, 1	1.5, 1.5	2, 2
0.7	0.5, 0.5	1, 1	1.3, 1.3	1.6, 1.6
0.8	0.5, 0.5	1, 1	1.3, 1.3	1.6, 1.6
1.0	0.5, 0.5	1, 1	1.2, 1.2	1.5, 1.5
5.0	0.8, 0.8	1.5, 1.5	1.5, 1.5	0, 0

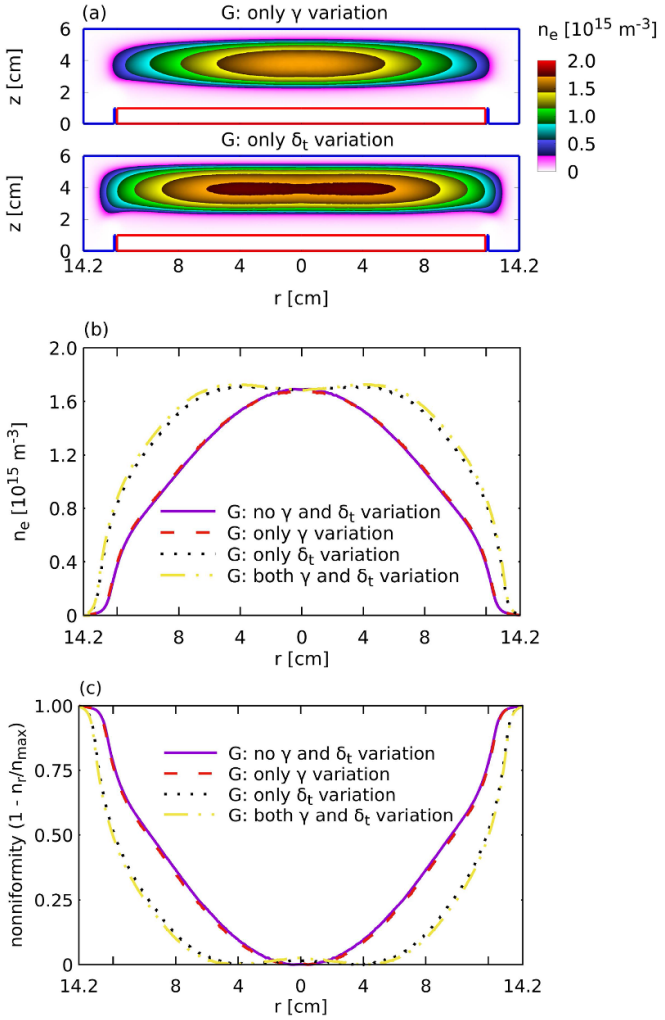

Figure 4. 2D spatial distributions of the time-averaged electron density for the cases where only a radial γ- or δ_t-coefficient variation is performed at the grounded electrode (a), radial distributions of time averaged electron density (b), and radial nonuniformity $(1 - n_r/n_{max})$ (c) at $z = 3.5$ cm with different surface coefficients at the grounded electrode. The gas pressure is 0.6 Pa, the other discharge conditions are the same as in figure 3.

To identify the respective effect of γ-electrons and electron induced surface processes on the plasma uniformity improvement at low pressures, figure 4 shows the 2D spatially resolved and time-averaged electron density, radial electron density profile at $z = 3.5$ cm and the corresponding non-uniformity for the cases where only a radial γ-coefficient variation and only a δ_t-coefficient variation is performed at the grounded electrode at 0.6 Pa. The respective γ and δ_t-coefficient settings at the different radial regions are the same as in the 0.6 Pa case listed in table 1, but only one of the two surface coefficients is varied and the other coefficient remains unchanged at γ_{SiO_2} or δ_{SiO_2}. The radial electron density and nonuniformity at $z = 3.5$ cm for the cases with both and without γ- and δ_t-coefficient variation are also shown in figures 4(b) and (c) as a reference. Compared to the case where no surface coefficient variation is done, the density profile is hardly changed in the case where only the γ-coefficient is varied. However, only varying the δ_t-coefficient radially can effectively improve the plasma uniformity. The density profile in this case is close to the case where both γ- and δ_t-coefficient variations are set at the grounded electrode. Therefore, the δ_t-electrons (including the δ-electrons and reflected electrons) are identified to play the major role in improving the plasma uniformity at low pressure conditions. In fact, this effect is mainly attributed to the geometrical asymmetry of the reactor, since in this case a large sheath is formed at the powered electrode while a small sheath is generated at the grounded electrode. Thus, ions bombard the grounded electrode with low energies, which results in very low γ-coefficients at this electrode (cf figure 2). Therefore, only a few γ-electrons will be emitted, even if the γ-coefficient is increased by some extent at the electrode edges in the surface variation case. These γ-electrons cannot contribute much to the ionization and do not significantly enhance the plasma density. However, the small sheath at the grounded electrode leads to an enhanced δ-electron emission and electron reflection at this electrode, since the energetic electrons accelerated near the powered electrode during the sheath expansion can overcome this low sheath potential and bombard the grounded electrode at relatively high energies, which leads to a high δ_t-coefficient at the grounded electrode. In this scenario, radially varying the δ_t-coefficient at the grounded electrode can effectively change the local electron yields, ionization dynamics and plasma density in the respective region.

The axially and temporally resolved total ionization rates at different radial regions at 0.6 Pa for the uniform SiO_2 surface coefficient case and for the radially varying surface coefficient case are shown in figure 5. Due to the geometrical asymmetry, a DC self-bias of -125 V is generated in the case of uniform SiO_2 surface coefficients at the grounded electrode. A large sheath is formed at the powered electrode, by which the electrons are accelerated strongly during the local sheath

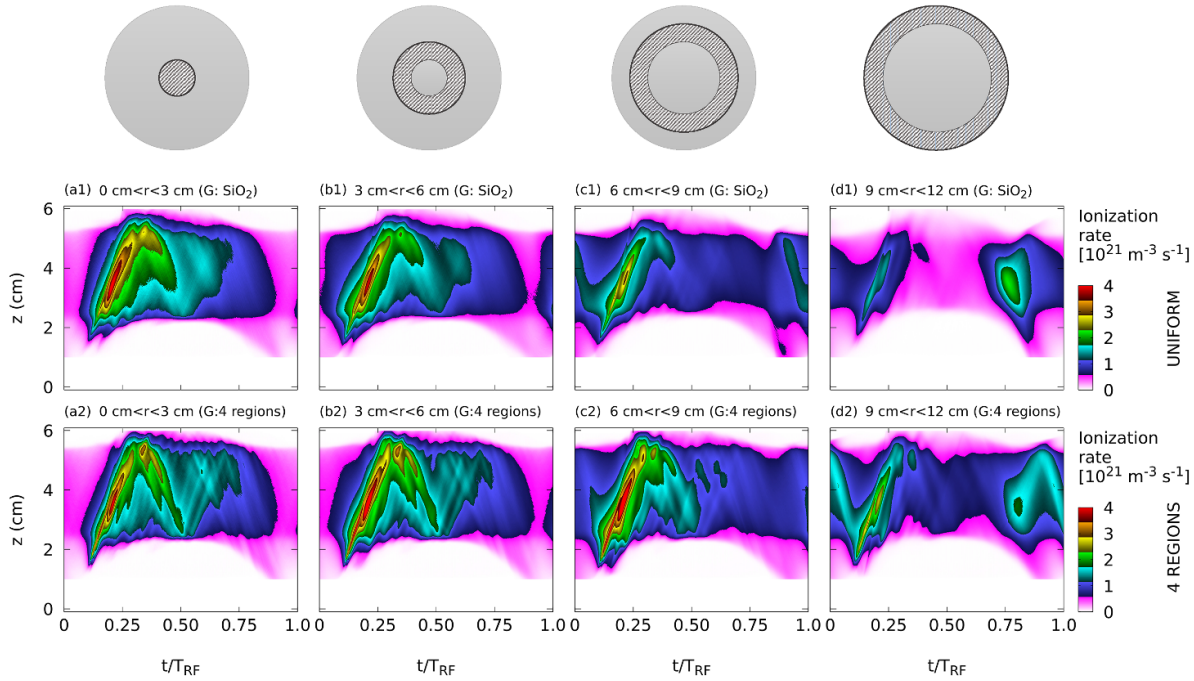

Figure 5. Axially and temporally resolved plots of the total ionization rate for uniform SiO_2 surface coefficients at the grounded electrode (first row) and radially varying surface coefficients at the grounded electrode (second row). The results were obtained by averaging the data in the radial direction within the region $0 < r < 3$ cm (first column), 3 cm $< r < 6$ cm (second column), 6 cm $< r < 9$ cm (third column), and 9 cm $< r < 12$ cm (fourth column), respectively, as indicated by the schematics at the top of the figure. The active surface of the powered electrode is situated at $z = 1$ cm. The gas pressure is 0.6 Pa. The other discharge conditions are the same as in figure 3.

expansion, resulting in the generation of energetic electron beams which lead to strong ionization in the bulk region. Some of these electrons bombard the grounded electrode at high energies during its sheath collapse and induce δ-electron emission/electron reflection. As shown in the figure, strong ionization is induced by the emitted and reflected electrons at $0.3 < t/T_{RF} < 0.5$. From the center to the edge region, the ionization rate during the sheath expansion at the powered electrode gradually decreases, since the electron density decreases as a function of radial position. However, a stronger ionization within the region 9 cm $< r <$ 12 cm forms during the sheath collapse at the powered electrode, when the sheath expands at the grounded electrode. This ionization peak is caused by the edge effect, i.e. strong electron heating by the superposed sheaths at the top electrode and at the sidewall at the top corners of the reactor, that expand simultaneously. Due to the non-local electron dynamics at 0.6 Pa, these electrons penetrate toward the center region and do not form a local plasma density peak at the edges of the reactor at this low pressure.

Radially varying the surface coefficients at the grounded electrode leads to a larger DC self-bias of -178 V, since more electrons are emitted/reflected at the grounded electrode and a smaller sheath is required to increase the electron bombardment at this electrode to balance the positive ion flux on time average [115]. The larger sheath at the powered electrode leads to a more pronounced self-excitation of the plasma series resonance [116–119] and to the generation of multiple energetic electron beams during its expansion phase [120]. Due to the reduced surface coefficients at $0 < r < 3$ cm, the ionization rate is slightly decreased in figure 5(a2) compared to (a1). However, the ionization is strongly enhanced at the regions $r > 3$ cm by the larger surface coefficients, which finally results in a higher plasma density near the sidewall and a better uniformity. In figure 5(d2), an evident energetic electron beam is observed during $0.75 < t/T_{RF} < 1.2$, which is formed in the bottom trench at the edge of the reactor (see figure 1) during the sheath expansion at the grounded electrode, then penetrates upwards into the bulk and is finally reflected by the sheath at the top grounded electrode. Since both the electron density and the surface coefficients are higher at large radial positions, this effect is more apparent in figure 5(d2) compared to figure 5(d1).

Figure 4 has shown that at low pressures the electron induced electron yields play the major role in improving the plasma uniformity by radially varying the surface coefficients. To further understand this, in figures 6 and 7, we show the time-averaged current densities of emitted δ-electrons and of elastically reflected electrons, respectively, at the different radial regions of the powered and grounded electrodes in the case of uniform SiO_2 surface coefficients and radially varying surface coefficients (the second case in table 1) at 0.6 Pa. With uniform SiO_2 surface coefficients at the grounded electrode, the δ-electron emission is reduced along the grounded electrode due to the lower plasma density at the edges. However, at the powered electrode, a higher total δ-electron emission current density is observed at 6 cm $< r <$ 9 cm (figure 6(c1)) compared to the other regions, which is caused by the strong local energetic electron bombardment. These energetic electrons are formed at the top corner of the reactor during its sheath expansion. After being accelerated by the local sheath,

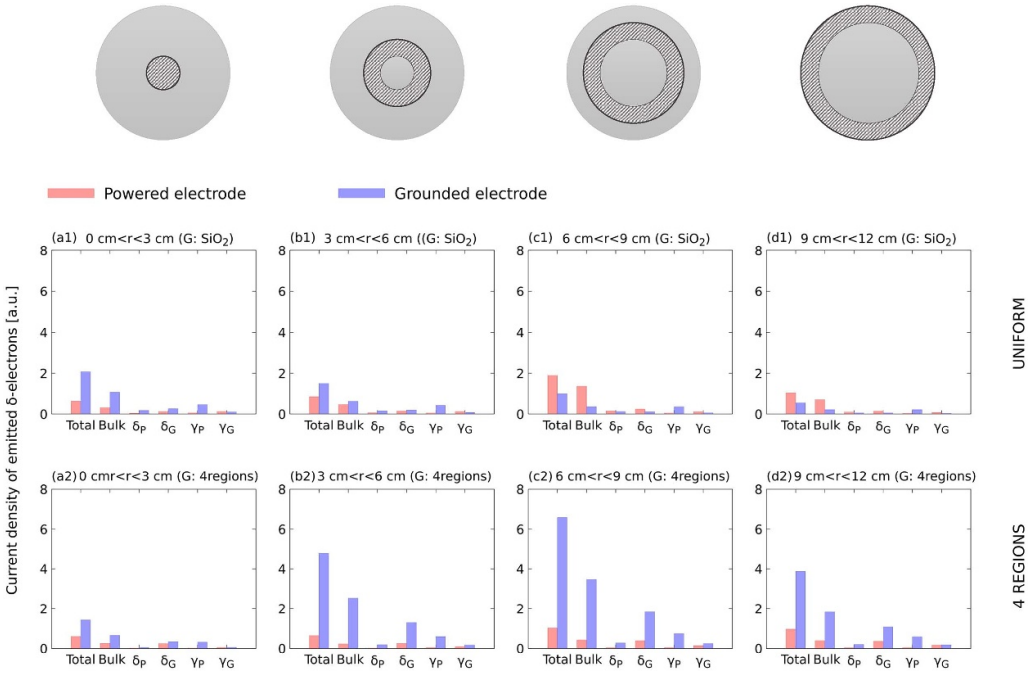

Figure 6. Time-averaged current densities of emitted δ-electrons induced by different electron groups at the respective radial regions (as indicated by the schematics at the top of the figure) of the powered and grounded electrodes in the cases of uniform SiO_2 surface coefficients (first row) and radially varying surface coefficients (second row) at the grounded electrode. In each panel, 'Bulk','δ_P','δ_G','γ_P' and 'δ_G' represent the current densities of emitted δ-electrons induced by bulk electrons, δ-electrons emitted at the powered electrode, δ-electrons emitted at the grounded electrode, γ-electrons emitted at the powered electrode, and γ-electrons emitted at the grounded electrode, respectively. The gas pressure is 0.6 Pa. The other discharge conditions are the same as in figure 3.

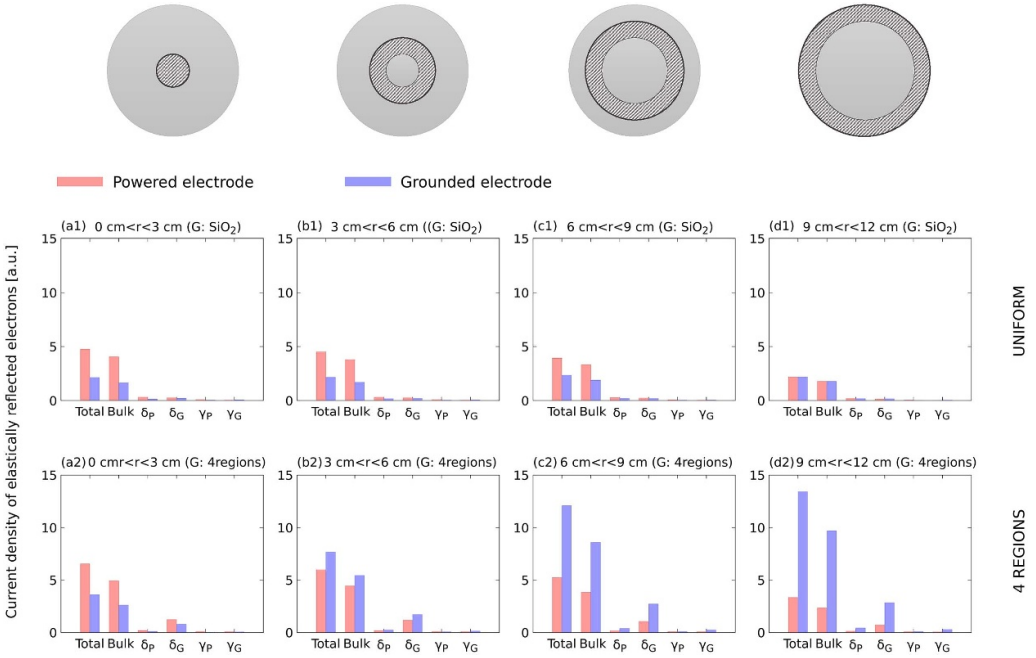

Figure 7. Time-averaged current densities of elastically reflected electrons induced by different electron groups at the respective radial regions (as indicated by the schematics at the top of the figure) of the powered and grounded electrodes in the cases of uniform SiO_2 surface coefficients (first row) and radially varying surface coefficients (second row) at the grounded electrode. The gas pressure is 0.6 Pa. The other discharge conditions are the same as in figure 3.

these electrons penetrate into the bulk at a specific angle and bombard the powered electrode within 6 cm $< r <$ 9 cm. The high δ-electron emission current at 6 cm $< r <$ 9 cm is largely reduced in the case of varying surface coefficients, since the sheath at the grounded electrode is much smaller and the electron heating by the sheath expansion at the top corner

is weak. Most importantly, by radially increasing the surface coefficient, the δ-electron emission at the grounded electrode is greatly enhanced within $r > 3$ cm, which increases the ionization rate and contributes to an augmented plasma density at the edges of the reactor. It is found that the bulk electrons are the main source of the δ-electron emission at the grounded electrode, i.e. the bulk electrons accelerated during the sheath expansion at the powered electrode bombard the grounded electrode during its collapse and induce δ-electron emission and electron reflection. Besides this, since a high number of δ-electrons is emitted at the grounded electrode, these δ-electrons can be further heated during the sheath expansion phase and are transported toward the powered electrode, where they are reflected by the sheath and again bombard the grounded electrode to induce more electron emission/reflection. Therefore, relatively high current densities induced by δ_G in figures 6(b2)–(d2) and figures 7(b2)–(d2) are observed.

Similar to the δ-electron emission, the electron reflection is also largely enhanced at the edges by radially increasing the surface coefficients. We note that the current density of the reflected electrons in figure 7 is even larger than the current density of emitted δ-electrons. This is because the electron bombardment energy is in the range where the elastic electron reflection coefficient is larger than the δ-electron emission coefficient, as shown in figure 2. Therefore, the reflected electrons play an even more important role for enhancing the ionization rate and plasma density near the sidewall compared with the δ-electrons at the discharge conditions studied here. The current density of inelastically reflected electrons shows a similar trend as that of the δ-electrons and elastically reflected electrons, but its amplitude is much lower due to the lower inelastic electron reflection coefficient. We, therefore, do not show it here.

We note, that in reactive plasmas deposition on boundary surfaces can occur. This might change the radial variation of surface coefficients and its effects on plasma uniformity. However, clear understandings on this must be obtained by further investigations and for specific discharge conditions (pressure, gases, reactor geometry). The 'proof of principle' findings in this work aimed at a fundamental understanding of how and why radially varying surface materials affect the radial plasma uniformity at low pressure and can help to improve it significantly. Moreover, since surface material variations occur naturally in many commercial reactors, our results help to understand their operations.

4. Conclusions

Using 2d3v PIC/MCC simulations we examined the effects of radially varying surface coefficients on the plasma uniformity in a geometrically asymmetric CCP discharge at low pressures ranging from 0.5 Pa to 5 Pa in argon gas. This study was motivated by (i) the fact that radial surface material variations commonly exist in CCP sources used in industry, but their effects are not understood, and (ii) the fact that improving the uniformity of CCPs becomes increasingly important due to the demand of large area etching and deposition for reducing the production cost. Radial surface material variation can be a promising method for improving the plasma uniformity keeping other discharge conditions unchanged.

Due to the lack of energy-dependent surface coefficients for different surface materials, the radial surface coefficient variation is realized by using the SiO_2 surface coefficients as base values and changing these radially by multiplying them by a factor ranging from 0 to 2. We note that according to previous studies [89–91, 121–123], the resulting coefficients are in a reasonable range resembling the presence of different surface materials qualitatively. For instance, according to [90, 122, 124], the total electron induced electron emission (including electron reflection and electron induced SEE) coefficients of Al_2O_3 and SiC materials are 1.5 to 2 times that of SiO_2 surfaces, while metals and some compounds such as Cu and Cu_2O have lower electron induced electron emission coefficients than SiO_2. Under the discharge conditions studied in this work, we found that these electron induced surface processes play the dominant role in changing the plasma uniformity through radial surface material variations.

The simulation results showed that at very low pressures, a center-high plasma density profile forms in case of uniform SiO_2 surface coefficients at both electrodes. By radially increasing the surface coefficients from the center to the edge region of the grounded electrode, the density at the radial edges can be enhanced and the plasma uniformity can be improved at both electrodes. At 5 Pa, a high density peak appears near the edges of the reactor due to the edge effect. In this case, by reducing the surface coefficients at the edges to zero and increasing them at 3 cm $\leqslant r <$ 9 cm a uniform density profile can be achieved.

The effects of the γ-coefficient and the electron induced electron emission and reflection coefficient, δ_t, were studied in detail at a specific pressure of 0.6 Pa. It was found that only varying the γ-coefficient at the grounded electrode can hardly change the density profile, while radially increasing δ_t can effectively enhance the density at the edges of the reactor and improve the plasma uniformity. From the current densities of the emitted δ-electrons and of the elastically reflected electrons as well as from the spatio-temporally resolved ionization rate plots at the respective radial regions of the reactor, we found that by increasing the surface coefficients at large radial positions, more electrons are emitted/reflected at the edge region of the reactor, leading to a high ionization rate near the edges which contributes to a more uniform plasma density. These emitted/reflected electrons are mainly induced by bulk electrons accelerated during the sheath expansion at the powered electrode, which then penetrate into the bulk region and finally bombard the grounded electrode during its sheath collapse at relatively high energies. Due to the higher elastic reflection coefficient at these electron bombardment energies, the electron elastic reflection is more prominent than the δ-electron emission and inelastic electron reflection. Thus, these elastically reflected electrons play the major role for improving the plasma uniformity at the discharge conditions studied.

Our results show that radial variations of the boundary surface material have significant effects on the radial plasma density profile in CCPs and should be taken into account in

simulations of such reactors to obtain realistic results. Radially tailoring the surface material at the grounded electrode, while leaving the wafer (located on the powered electrode) unchanged, can effectively improve the plasma uniformity at low pressures, which could be a potentially promising method to be adopted in industrial applications. We note that at pressures of about 8 Pa, this method became inefficient due to the reduced electron mean free path, since much less electrons can bombard the grounded electrode at high energies and induce electron emission as well as reflection. However, we expect the surface coefficient variation to again play a significant role for improving the uniformity at even higher pressures, at which the γ-mode is present. Then the radial variation of γ rather than δ_t should be important. Such studies are expected to be conducted in the future.

Data availability statement

The data that support the findings of this study are available at https://rdpcidat.rub.de/node/627.

Acknowledgments

This work was supported by the National Natural Science Foundation of China (No. 12020101005, 11975067), by the German Research Foundation in the frame of the project 'Electron heating in capacitive RF plasmas based on moments of the Boltzmann equation: from fundamental understanding to knowledge based process control' (No. 428942393), and by the National Office for Research, Development and Innovation of Hungary (NKFIH) via Grants K-134462, K-132158.

ORCID iDs

Li Wang https://orcid.org/0000-0002-3106-2779
Peter Hartmann https://orcid.org/0000-0003-3572-1310
Zoltán Donkó https://orcid.org/0000-0003-1369-6150
Yuan-Hong Song https://orcid.org/0000-0001-5712-9241
Julian Schulze https://orcid.org/0000-0001-7929-5734

References

[1] Lieberman M A and Lichtenberg A J 2005 *Principles of Plasma Discharges and Materials Processing* 2nd edn (New York: Wiley)
[2] Chabert P and Braithwaite N 2011 *Physics of Radio-Frequency Plasmas* (Cambridge: Cambridge University Press)
[3] Huang S, Shim S, Nam S K and Kushner M J 2020 *J. Vac. Sci. Technol.* A **38** 023001
[4] Huang S, Huard C, Shim S, Nam S K, Song I C, Lu S and Kushner M J 2019 *J. Vac. Sci. Technol.* A **37** 031304
[5] Kushner M J 1985 *J. Appl. Phys.* **58** 4024–31
[6] Hartmann P, Korolov I, Escandón-López J, van Gennip W, Buskes K and Schulze J 2022 *Plasma Sources Sci. Technol.* **31** 055017
[7] Booth J P 1999 *Plasma Sources Sci. Technol.* **8** 249–57
[8] Kaler S S, Lou Q, Donnelly V M and Economou D J 2017 *J. Phys. D: Appl. Phys.* **50** 234001
[9] Booth J P, Cunge G, Chabert P and Sadeghi N 1999 *J. Appl. Phys.* **85** 3097–107
[10] Korolov I, Donkó Z, Hübner G, Bischoff L, Hartmann P, Gans T, Liu Y, Mussenbrock T and Schulze J 2019 *Plasma Sources Sci. Technol.* **28** 094001
[11] Perret A, Chabert P, Jolly J and Booth J P 2005 *Appl. Phys. Lett.* **86** 021501
[12] Liu Y X, Liang Y S, Wen D Q, Bi Z H and Wang Y N 2015 *Plasma Sources Sci. Technol.* **24** 025013
[13] Turner M M and Chabert P 2007 *Plasma Sources Sci. Technol.* **16** 364–71
[14] Gans T, Schulze J, O'Connell D, Czarnetzki U, Faulkner R, Ellingboe A R and Turner M M 2006 *Appl. Phys. Lett.* **89** 261502
[15] Heil B G, Czarnetzki U, Brinkmann R P and Mussenbrock T 2008 *J. Phys. D: Appl. Phys.* **41** 165202
[16] Lee J K, Babaeva N, Kim H C, Manuilenko O and Shon J W 2004 *IEEE Trans. Plasma Sci.* **32** 47–53
[17] Kitajima T, Takeo Y, Petrović Z L and Makabe T 2000 *Appl. Phys. Lett.* **77** 489–91
[18] Kitajima T, Takeo Y and Makabe T 1999 *J. Vac. Sci. Technol.* A **17** 2510–6
[19] Boyle P C, Ellingboe A R and Turner M M 2004 *Plasma Sources Sci. Technol.* **13** 493–503
[20] Boyle P C, Ellingboe A R and Turner M M 2004 *J. Phys. D: Appl. Phys.* **37** 697–701
[21] Schulze J, Gans T, O'Connell D, Czarnetzki U, Ellingboe A R and Turner M M 2007 *J. Phys. D: Appl. Phys.* **40** 7008–18
[22] Georgieva V, Bogaerts A and Gijbels R 2004 *Phys. Rev.* E **69** 026406
[23] Zhang Y, Kushner M J, Sriraman S, Marakhtanov A, Holland J and Paterson A 2015 *J. Vac. Sci. Technol.* A **33** 031302
[24] Zhang Y, Kushner M J, Moore N, Pribyl P and Gekelman W 2013 *J. Vac. Sci. Technol.* A **31** 061311
[25] Takagi S, Chikata T and Sekine M 2020 *Jpn. J. Appl. Phys.* **60** SAAB07
[26] Rauf S and Balakrishna A 2017 *J. Vac. Sci. Technol.* A **35** 021308
[27] Czarnetzki U, Schulze J, Schüngel E and Donkó Z 2011 *Plasma Sources Sci. Technol.* **20** 024010
[28] Schulze J, Schüngel E, Donkó Z and Czarnetzki U 2011 *Plasma Sources Sci. Technol.* **20** 015017
[29] Schulze J, Schüngel E, Donkó Z and Czarnetzki U 2010 *Plasma Sources Sci. Technol.* **19** 045028
[30] Liu Y X, Zhang Q Z, Jiang W, Hou L J, Jiang X Z, Lu W Q and Wang Y N 2011 *Phys. Rev. Lett.* **107** 055002
[31] Derzsi A, Schüngel E, Donkó Z and Schulze J 2015 *Open Chem.* **13** 346–61
[32] Schuengel E, Schulze J, Donko Z and Czarnetzki U 2011 *Phys. Plasmas* **18** 013503
[33] Wen D Q, Zhang Q Z, Jiang W, Song Y, Bogaerts A and Wang Y N 2014 *J. Appl. Phys.* **115** 233303
[34] Donkó Z, Derzsi A, Vass M, Schulze J, Schuengel E and Hamaguchi S 2018 *Plasma Sources Sci. Technol.* **27** 104008
[35] Derzsi A, Horváth B, Korolov I, Donkó Z and Schulze J 2019 *J. Appl. Phys.* **126** 043303
[36] Derzsi A, Bruneau B, Gibson A R, Johnson E, O'Connell D, Gans T, Booth J P and Donkó Z 2017 *Plasma Sources Sci. Technol.* **26** 034002
[37] Lafleur T 2015 *Plasma Sources Sci. Technol.* **25** 013001
[38] Lafleur T, Delattre P A, Johnson E V and Booth J P 2013 *Plasma Phys. Control. Fusion* **55** 124002
[39] Lafleur T, Boswell R W and Booth J P 2012 *Appl. Phys. Lett.* **100** 194101

[40] Brandt S *et al* 2016 *Plasma Sources Sci. Technol.* **25** 045015
[41] Wang L, Hartmann P, Donkó Z, Song Y H and Schulze J 2021 *Plasma Sources Sci. Technol.* **30** 054001
[42] Hartmann P *et al* 2020 *Plasma Sources Sci. Technol.* **29** 075014
[43] Hartmann P *et al* 2021 *J. Phys. D: Appl. Phys.* **54** 255202
[44] Zhang P, Zhang L and Xu L 2020 *Plasma Process Polym.* **17** 2000014
[45] Krüger F, Wilczek S, Mussenbrock T and Schulze J 2019 *Plasma Sources Sci. Technol.* **28** 075017
[46] Lieberman M A, Lichtenberg A J and Savas S E 1991 *IEEE Trans. Plasma Sci.* **19** 189–96
[47] Kushner M J 2003 *J. Appl. Phys.* **94** 1436–47
[48] Yang S, Zhang Y, Wang H, Cui J and Jiang W 2017 *Plasma Process Polym.* **14** 1700087
[49] Yang S, Chang L, Zhang Y and Jiang W 2018 *Plasma Sources Sci. Technol.* **27** 035008
[50] Oberberg M, Engel D, Berger B, Wölfel C, Eremin D, Lunze J, Brinkmann R P, Awakowicz P and Schulze J 2019 *Plasma Sources Sci. Technol.* **28** 115021
[51] Oberberg M, Kallähn J, Awakowicz P and Schulze J 2018 *Plasma Sources Sci. Technol.* **27** 105018
[52] Oberberg M, Berger B, Buschheuer M, Engel D, Woelfel C, Eremin D, Lunze J, Brinkmann R P, Awakowicz P and Schulze J 2020 *Plasma Sources Sci. Technol.* **29** 075013
[53] Wang L, Vass M, Donkó Z, Hartmann P, Derzsi A, Song Y H and Schulze J 2021 *Plasma Sources Sci. Technol.* **30** 10LT01
[54] Wang L, Wen D Q, Hartmann P, Donkó Z, Derzsi A, Wang X F, Song Y H, Wang Y N and Schulze J 2020 *Plasma Sources Sci. Technol.* **29** 105004
[55] Wang L, Vass M, Donkó Z, Hartmann P, Derzsi A, Song Y H and Schulze J 2022 *Plasma Sources Sci. Technol.* **31** 06LT01
[56] Sun J Y, Zhang Q Z, Liu J R, Song Y H and Wang Y N 2020 *Plasma Sources Sci. Technol.* **29** 114002
[57] Zheng B, Wang K, Grotjohn T, Schuelke T and Fan Q H 2019 *Plasma Sources Sci. Technol.* **28** 09LT03
[58] Patil S, Sharma S, Sengupta S, Sen A and Kaganovich I 2022 *Phys. Rev. Res.* **4** 013059
[59] Zhang Q Z, Sun J Y, Lu W Q, Schulze J, Guo Y Q and Wang Y N 2021 *Phys. Rev.* E **104** 045209
[60] Trieschmann J, Shihab M, Szeremley D, Elgendy A E, Gallian S, Eremin D, Brinkmann R P and Mussenbrock T 2013 *J. Phys. D: Appl. Phys.* **46** 084016
[61] Turner M M, Hutchinson D A W, Doyle R A and Hopkins M B 1996 *Phys. Rev. Lett.* **76** 2069–72
[62] You S J, Kim S S and Chang H Y 2004 *Appl. Phys. Lett.* **85** 4872–4
[63] Lieberman M A, Booth J P, Chabert P, Rax J M and Turner M M 2002 *Plasma Sources Sci. Technol.* **11** 283–93
[64] Lieberman M A, Lichtenberg A J, Kawamura E and Marakhtanov A M 2015 *Plasma Sources Sci. Technol.* **24** 055011
[65] Wen D Q, Kawamura E, Lieberman M A, Lichtenberg A J and Wang Y N 2016 *Plasma Sources Sci. Technol.* **26** 015007
[66] Wen D Q, Kawamura E, Lieberman M A, Lichtenberg A J and Wang Y N 2017 *J. Phys. D: Appl. Phys.* **50** 495201
[67] Zhao K, Wen D Q, Liu Y X, Lieberman M A, Economou D J and Wang Y N 2019 *Phys. Rev. Lett.* **122** 185002
[68] Sansonnens L, Howling A A and Hollenstein C 2006 *Plasma Sources Sci. Technol.* **15** 302–13
[69] Liu Y X, Zhang Q Z, Zhao K, Zhang Y R, Gao F, Song Y H and Wang Y N 2022 *Chin. Phys.* B **31** 085202
[70] Sansonnens L and Schmitt J 2003 *Appl. Phys. Lett.* **82** 182–4
[71] Schmidt H, Sansonnens L, Howling A A, Hollenstein C, Elyaakoubi M and Schmitt J P M 2004 *J. Appl. Phys.* **95** 4559–64
[72] Chabert P, Raimbault J L, Rax J M and Perret A 2004 *Phys. Plasmas* **11** 4081–7
[73] Chen Z, Kenney J, Rauf S, Collins K, Tanaka T, Hammond N and Kudela J 2011 *IEEE Trans. Plasma Sci.* **39** 2526–7
[74] Yang Y and Kushner M J 2010 *J. Phys. D: Appl. Phys.* **43** 152001
[75] Schmidt N, Schulze J, Schüngel E and Czarnetzki U 2013 *J. Phys. D: Appl. Phys.* **46** 505202
[76] Wang L, Hartmann P, Donkó Z, Song Y H and Schulze J 2021 *J. Vac. Sci. Technol.* A **39** 063004
[77] Ďurian J, Hartmann P, Matejčík Š, Gibson A R and Donkó Z 2022 *Plasma Sources Sci. Technol.* **31** 095001
[78] Ohtsu Y, Matsumoto N, Schulze J and Schuengel E 2016 *Phys. Plasmas* **23** 033510
[79] Zhao K, Su Z X, Liu J R, Liu Y X, Zhang Y R, Schulze J, Song Y H and Wang Y N 2020 *Plasma Sources Sci. Technol.* **29** 124001
[80] Schüngel E, Mohr S, Schulze J and Czarnetzki U 2015 *Appl. Phys. Lett.* **106** 054108
[81] Lim Y M, Park S Y, He Y, Hong Y H and Chung C W 2022 *J. Vac. Sci. Technol.* A **40** 063003
[82] Donkó Z, Schulze J, Hartmann P, Korolov I, Czarnetzki U and Schüngel E 2010 *Appl. Phys. Lett.* **97** 081501
[83] Küllig C, Dittmann K, Wegner T G, Sheykin I E, Matyash K, Loffhagen D, Schneider R and Meichsner J 2012 Dynamics and electronegativity of oxygen RF plasmas *Contrib. to Plasma Phys.* **52** 836
[84] Vass M, Derzsi A, Schulze J and Donko Z 2021 Electron tennis driven by radio-frequency electric fields in low-pressure plasma sources *Plasma Sources Sci. Technol.* **30** 03LT04
[85] Proto A and Gudmundsson J T 2018 *Atoms* **6** 65
[86] Schulze J, Donkó Z, Schüngel E and Czarnetzki U 2011 *Plasma Sources Sci. Technol.* **20** 045007
[87] Lafleur T, Chabert P and Booth J P 2013 *J. Phys. D: Appl. Phys.* **46** 135201
[88] Korolov I, Derzsi A, Donkó Z and Schulze J 2013 *Appl. Phys. Lett.* **103** 064102
[89] Phelps A V and Petrovic Z L 1999 *Plasma Sources Sci. Technol.* **8** R21–R44
[90] Barral S, Makowski K, Peradzyński Z, Gascon N and Dudeck M 2003 *Phys. Plasmas* **10** 4137–52
[91] Horváth B, Daksha M, Korolov I, Derzsi A and Schulze J 2017 *Plasma Sources Sci. Technol.* **26** 124001
[92] Demidov V I, Adams S F, Kaganovich I D, Koepke M E and Kurlyandskaya I P 2015 *Phys. Plasmas* **22** 104501
[93] Daksha M, Derzsi A, Wilczek S, Trieschmann J, Mussenbrock T, Awakowicz P, Donkó Z and Schulze J 2017 *Plasma Sources Sci. Technol.* **26** 085006
[94] Daksha M, Derzsi A, Mujahid Z, Schulenberg D, Berger B, Donkó Z and Schulze J 2019 *Plasma Sources Sci. Technol.* **28** 034002
[95] Derzsi A, Korolov I, Schüngel E, Donkó Z and Schulze J 2015 *Plasma Sources Sci. Technol.* **24** 034002
[96] Gudmundsson J T, Krek J, Wen D Q, Kawamura E and Lieberman M A 2021 *Plasma Sources Sci. Technol.* **30** 125011
[97] Voloshin D G, Mankelevich Y A, Proshina O V and Rakhimova T V 2017 *Plasma Process Polym.* **14** 1600119
[98] Horváth B, Schulze J, Donkó Z and Derzsi A 2018 *J. Phys. D: Appl. Phys.* **51** 355204
[99] Schulenberg D A, Korolov I, Donkó Z, Derzsi A and Schulze J 2021 *Plasma Sources Sci. Technol.* **30** 105003
[100] Mussenbrock T, Hemke T, Ziegler D, Brinkmann R P and Klick M 2008 *Plasma Sources Sci. Technol.* **17** 025018
[101] Donkó Z 2011 *Plasma Sources Sci. Technol.* **20** 024001
[102] Donkó Z, Derzsi A, Vass M, Horváth B, Wilczek S, Hartmann B and Hartmann P 2021 *Plasma Sources Sci. Technol.* **30** 095017

[103] COP database 2020 (available at: www.lxcat.net) (Accessed 10 January)
[104] McEachran R and Stauffer A 2014 *Eur. Phys. J.* D **68** 153
[105] Hayashi database 2020 (available at: www.lxcat.net) (Accessed on 10 January)
[106] Hayashi M 2003 Bibliography of electron and photon cross sections with atoms and molecules published in the 20th century — argon *Technical Report NIFS-DATA-072* (National Institute for Fusion Science Toki, GIFU, 509-5292, Japan) (available at: www.nifs.ac.jp/report/NIFS-DATA-072.pdf)
[107] Phelps A V 1991 *J. Phys. Chem. Ref. Data* **20** 557–73
[108] Phelps A V 1994 *J. Appl. Phys.* **76** 747–53
[109] Okhrimovskyy A, Bogaerts A and Gijbels R 2002 *Phys. Rev.* E **65** 037402
[110] Buschhaus R, Prenzel M and von Keudell A 2022 *Plasma Sources Sci. Technol.* **31** 025017
[111] Sobolewski M A 2021 *Plasma Sources Sci. Technol.* **30** 025004
[112] Braginsky O, Kovalev A, Lopaev D, Proshina O, Rakhimova T, Vasilieva A, Voloshin D and Zyranov S 2012 *J. Phys.* D **45** 015201
[113] Evans D 1984 *Parallel Comput.* **1** 3–18
[114] Konstantinidis E and Cotronis Y 2012 Accelerating the red/black SOR method using GPUs with CUDA *Parallel Processing and Applied Mathematics* ed R Wyrzykowski J Dongarra K WKarczewski and J Waśniewski (Berlin: Springer) pp 589–98
[115] Schulze J, Schuengel E, Donko Z and Czarnetzki U 2010 *J. Phys.* D **43** 225201
[116] Wilczek S *et al* 2016 *Phys. Plasmas* **23** 063514
[117] Schulze J, Kampschulte T, Luggenhölscher D and Czarnetzki U 2007 *J. Phys.: Conf. Ser.* **86** 012010
[118] Czarnetzki U, Mussenbrock T and Brinkmann R P 2006 *Phys. Plasmas* **13** 123503
[119] Donkó Z, Schulze J, Czarnetzki U and Luggenhölscher D 2009 *Appl. Phys. Lett.* **94** 131501
[120] Berger B, You K, Lee H C, Mussenbrock T, Awakowicz P and Schulze J 2018 *Plasma Sources Sci. Technol.* **27** 12LT02
[121] Campanell M D 2013 *Phys. Rev.* E **88** 033103
[122] Seiler H 1983 *J. Appl. Phys.* **54** R1–R18
[123] Bronshtein I M and Fraiman B S (available at: www.osti.gov/biblio/4160985)
[124] Derzsi A, Horváth B, Donkó Z and Schulze J 2020 *Plasma Sources Sci. Technol.* **29** 074001